H/D Isotopic Exchange in Water Interactions with the Ferroelectric Copolymer: Poly(vinylidene fluoride−trifluoroethylene) (70%:30%)

Luis G. Rosa,[†] I. N. Yakovkin,[‡] and P. A. Dowben*,[†]

Department of Physics and Astronomy and the Center for Materials Research and Analysis, University of Nebraska, Lincoln, Nebraska 68588-0111, and Institute of Physics of National Academy of Sciences of Ukraine, Prospect Nauki 46, Kiev 03028, Ukraine

Received: April 5, 2005; In Final Form: May 25, 2005

For both water and heavy water adsorption and absorption on crystalline poly(vinylidene fluoride with trifluoroethylene (30%)), P(VDF-TrFE 70:30), two distinctly different adsorption sites have been identified by thermal desorption spectroscopy. One adsorbed water species resembles ice and there is also an absorbed water species that interacts more strongly with the polymer thin film, and in addition, there is a polymer surface (polymer to ice interface) water species. We find that there is H/D exchange between the water or heavy water molecules and the ferroelectric polymer (largely $-(CH_2-CF_2)-$), particularly at the polymer surface.

1. Introduction

The H/D exchange reaction $H_2O + D_2O \rightarrow 2HDO$, between water molecules,[1] and within ice,[2−4] between molecular hydrogen ($H_2 + D_2 \rightarrow 2HD$),[5] has been observed. H/D exchange reactions have also been found between dissimilar hydrogen containing molecules such as between small organic molecules and water,[6] water (and other small molecules) and proteins,[7] and DNA.[8] In all of these studies, the main mechanism is based on quantum tunneling of the atoms between each molecule on a hydrogen bond network.

Water adsorption on surfaces (and the formation of ice) has been a major part of surface science for decades[9,10] although there is not yet a corresponding level of understanding for water (or indeed any adsorbate) interaction with polymer surfaces.[11] Despite the complexities of polymer surface characterization, water has nevertheless been identified as a cause of molecular reorientation at polymer surfaces,[12−22] including the surface structure of fluorinated polymers.[24,25]

Water, while ubiquitous, does have a large dipole. This water dipole contributes to the complexity of water interaction with surfaces (and polymers). Water absorption is also known to change the dielectric properties of polymers, including copolymers of poly(vinylidene fluoride with trifluoroethylene),[26−28] suggesting an interaction between the dipole of water and the dipole of the ferroelectric[29−31] copolymers of poly(vinylidene fluoride). There is further experimental weight supporting possible strong interactions between water and a molecular ferroelectric from the observed steric effects in the thermal desorption of water from a ferroelectric polymer: the crystalline copolymer poly(vinylidene fluoride with trifluoroethylene (30%)), P(VDF-TrFE 70:30).[32] This interaction between the polymer surface and water[32] occurs in spite of a strong surface barrier to water absorption in the bulk,[26] but is not yet compelling proof of a dipole−dipole interaction between water and the ferroelectric. To further investigate the water interaction with the crystalline ferroelectric copolymer poly(vinylidene fluoride with trifluoroethylene (30%)), P(VDF-TrFE 70:30), we have investigated the hydrogen/deuterium isotopic exchange between water and this crystalline polymer ferroelectric.

2. Experimental Section

Copolymers poly(vinylidene fluoride with trifluoroethylene) have a number of advantages for the surface scientist interests in adsorption, and absorption studies in that ultrathin crystalline films of these polymers can be formed: thin enough for sufficient thermal conductivity for thermal desorption experiments as described here. The Langmuir−Blodgett technique for fabricating the P(VDF-TrFE) films provides sufficient crystalline order for scanning tunneling microscopy,[33−37] low energy electron diffraction,[33−37] and even band structure mappings,[36−37] so that in many respects adsorbate interactions can be investigated in much the same way as traditional surface science studies undertaken on single-crystal metal surfaces. The crystalline ferroelectric copolymer poly(vinylidene fluoride with trifluoroethylene), P(VDF-TrFE 70:30), is also a rich system for the study of ferroelectricity[29−31] with well-ordered surface dipoles.[32−38]

The ultrathin ferroelectric films of a copolymer like 70% vinylidene fluoride with 30% trifluoroethylene, P(VDF-TrFE 70:30), were fabricated by Langmuir−Blodgett (LB) deposition technique on graphite substrates from the water subphase, which can produce films with a thickness ranging from 1 monolayer (1 ML ≈ 0.5 nm) to over 500 ML.[30−31] The bulk crystallinity has been confirmed by X-ray diffraction on films from 4 to 150 ML thick.[26,31−32,37]

Any residual water that may remain in the PVDF-TrFE film following fabrication is removed by vacuum annealing. The purity of our films, free from contamination, was ascertained by comparing the photoemission and high-resolution electron energy loss spectra from in situ vacuum evaporated PVDF films with films fabricated by Langmuir−Blodgett (LB) deposition techniques. Following the adsorption of water at 120 K, the

* Address correspondence to this author. Phone: 402-472-9838. Fax: 402-472-2879. E-mail: pdowben@unl.edu.
[†] University of Nebraska.
[‡] Institute of Physics of National Academy of Sciences of Ukraine.

10.1021/jp051737j CCC: $30.25
Published on Web 06/22/2005

presence of ice was confirmed with angle-resolved photoemission, in a separate ultrahigh vacuum system described in ref 38.

The thermal desorption studies were undertaken in an ultrahigh vacuum chamber with sample cooling to 120−135 K as described elsewhere.[32,39] The temperature was determined by using a calibrated chromel−alumel thermocouple. To perform the thermal desorption, a quadrupole mass spectrometer (Dycor) operated by the new Ametek software was differentially pump by an ion pump. The samples, nominally 25 and 35 molecular layers thick, were cleaned in ultrahigh vacuum by annealing at 110 °C before and after each scan for 30 min, which has proved to be an effective recipe in prior studies.[33−38] The heating rates for obtaining the thermal desorption spectra were 0.5 deg/s throughout this work. Water exposures are denoted in langmuirs, where 1 L = 10^{-6} Torr·s, with water or heavy water exposed to P(VDF-TrFE) at 120 to 135 K. Water and heavy water were ultrapure and deionized. Water and heavy water vapor were inserted into the ultrahigh vacuum chamber (UHV) through a leak valve.

3. Theoretical Models

To obtain a qualitative picture of the behavior of a (heavy) water molecule at the polymer surface, both structure optimization and molecular dynamics (MD) simulations were undertaken with use of the HyperChem code within a semiempirical (SE) quantum mechanical method,[40] which includes parametrization of overlap integrals in the framework of the restricted Hartree−Fock (RHF) method. The semiempirical calculational approach, with the PM3 parameter set, has been recognized as a sufficiently accurate and very efficient method for the estimation of favored structures of molecular systems, in particular polymers,[38,41−42] by minimization of total energy. While somewhat simplistic, this approach is also adequate for simulations modeling the evolution of molecular systems at finite temperatures by molecular dynamics methods, which take into account the molecular and atomic kinetic energies.

We have tested our semiempirical calculations against plane wave based density functional theory (DFT) methods within the Perdew−Burke−Ernzerhof (PBE) generalized gradient approximation,[43] as implemented in the CASTEP computer code[44] with regard to the polymer structure and the structure of the ice (three layer slab) on poly(vinylidene fluoride−trifluoroethylene) where the supercell dimensions were 20.0 Å × 10.481 Å. With an energy convergence for geometry relation of 2 × 10^{-5} eV per atom, qualitative agreement was obtained with the structures obtained with semiempirical methods. For example, the obtained optimized geometry of a free water molecule is characterized by a 107.7° H−O−H angle and a 0.95 Å H−O bond length, in excellent agreement with ab initio results, obtained with the RHF method by using various (STO-3G, 6-21G, 6-31G) basis sets. The dipole moment of the water molecule after geometry optimization within the semiempirical calculational method is 1.74 D, consistent with the range of values, from 1.71 to 2.20 D, as obtained with different basis sets, and with the value of 2.01 D obtained within DFT GGA. The same efficacy of the semiempirical calculational method holds also for an $H_2C{=}CF_2$ molecule, which is the main building block of the PVDF. Here optimization within semiempirical approximation results in a C−C distance of 1.337 Å, a C−H distance of 1.085 Å and a C−C−H angle of 120°. Hence, the semiempirical approximation has been found to be sufficient for purposes of modeling of behavior of the (heavy) water molecule near the P(VDF-TrFE) surface and in the film interior.

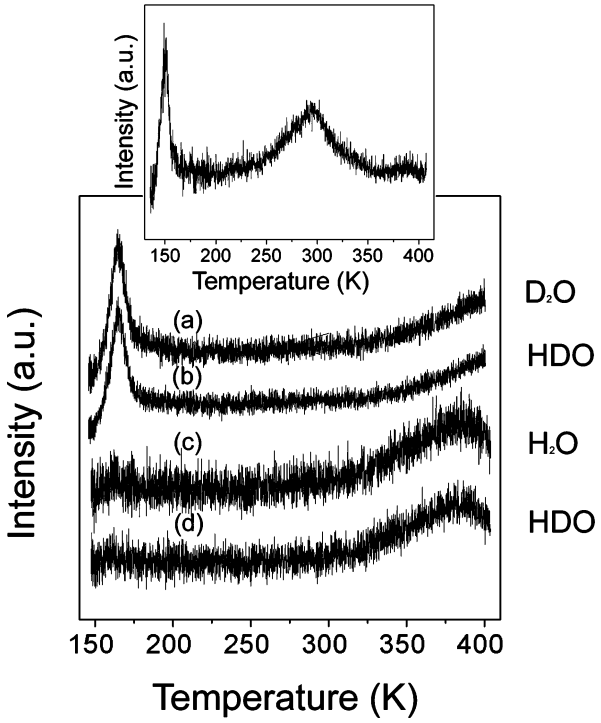

Figure 1. The 35 ML thick sample was expose to heavy water first; this figure shows thermal desorption spectra of heavy water and simultaneously measured HDO after the P(VDF-TrFE) sample has been exposed to 120 langmuirs of heavy water (spectra a and b, respectively). We also show the thermal desorption spectra of water and HDO (spectra c and d, respectively) after the film had been heavily deuterated by exposing the sample many times to heavy water. The latter thermal desorption spectra was taken after the deuterated P(VDF-TrFE) was exposed to 150 langmuirs at 130 K. To illustrate the thermal desorption peaks for both the water ice and absorbed water, the inset shows a thermal desorption spectra taken after 15 langmuirs water exposure to a thin, nominally 3 monolayer thick, P(VDF-TrFE) copolymer film.

Molecular dynamics simulations of movements of a water molecule close to the surface and in interior of the P(VDF-TrFE) films were performed with Newtonian mechanics on the potential energy surface calculated within the SE quantum mechanics method. Energy dissipation was taken into account by introducing the "constant temperature" mode (in practice, by adjusting the bath relaxation time, which simulates kinetic energy exchange with a thermostat). Within HyperChem, the obtained trajectories of water molecules can be visualized, which allows one to study the role of different starting conditions in the behavior of the molecule.

In simulations where the P(VDF-TrFE) chain structure and orientation was allowed to relax, in response to the proximity of a water molecule, the length of the two P(VDF-TrFE) chains was increased in the model calculations. This provided stability to the P(VDF-TrFE) films (with short chains, a reversible relaxation accompanying water absorption and desorption cannot be achieved), while the graphite substrate (whose influence was found to be insignificant, as discussed below) was removed. Both calculations maintained the 99 atoms in total, and a net optimization of the system, with various starting geometries, was undertaken.

4. Absorbed and Adsorbed Water

Consistent with prior studies,[32] following exposure of water or heavy water to crystalline thin films of P(VDF-TrFE 70:30) at 120−135 K, the thermal desorption spectra are characterized by two desorption peaks, as indicated in the inset to Figure 1.

The water ice species desorbs from the surface of the crystalline copolymer poly(vinylidene fluoride with trifluoroethylene (30%)), P(VDF-TrFE 70:30), in the vicinity of 160 K, while the absorbed water desorbs from P(VDF-TrFE 70:30) well above 300 K depending on film thickness, as has been observed previously.[32] The desorption temperature for absorbed water varies from approximately 300 K for a nominally 3 monolayer thick P(VDF-TrFE) film (shown in the inset to Figure 1) to 360 K for a nominally 25 monolayer thick P(VDF-TrFE) film and to 375 K for a nominally 35 monolayer thick P(VDF-TrFE) film.

The water ice thermal desorption peak, at 150−165 K, is not observed until P(VDF-TrFE) is exposed (at 120−135 K) to significant amounts of H_2O (250 L) or D_2O (50 L) and then annealed. This suggests[32] that some significant occupation of the more strongly bound water absorption sites in the near surface region must occur first. The ice, like weakly bound adsorbed water species, desorbs at only slightly higher temperatures for D_2O (about 165 K) than for H_2O (155 K), and the temperature for the desorption of this "ice" species depends little upon increasing exposure once P(VDF-TrFE) has been exposed to sufficient water or heavy water to observe this low temperature "ice" thermal desorption peak (i.e. this thermal desorption peak obeys nearly zero order desorption kinetics[45]). The absence of any P(VDF-TrFE) film thickness dependence, isotopic (water or heavy water) dependence, and only a slight difference in desorption temperature for D_2O versus H_2O indicate that this feature is indeed a result of desorption of a surface species akin to ice. With sufficient water exposure, there is enough water adsorption to obscure all of the photoemission features attributable to PVDF-TrFE,[46] so that only the three expected photoemission features of water are observed.

On the basis of the dependence of the high-temperature thermal desorption feature upon the P(VDF-TrFE) film thickness, it was suggested[32] that bulk diffusion of an absorbed phase of water affects the thermal desorption of water at high temperatures. The absorption of water is further supported by the effect of the adsorbate mass and the thermal desorption heating rate. The D_2O desorbs at an even higher temperature, more than 400K for a nominally 35 monolayer P(VDF-TrFE) film, than is observed for water (375 K for the same film), as indicated in Figure 1. If the desorption process involves bulk water diffusion to the surface, then the substantially heavier mass of D_2O versus H_2O could "delay" desorption to a higher temperature, as is observed. The desorption temperature was also affected by heating rate, with higher thermal desorption heating rates moving the desorption peak of the absorbed water to higher temperatures.

Because the P(VDF-TrFE) film melts in the vicinity of 180 °C, we have not been able to ascertain the exact desorption temperatures of the absorbed phase of D_2O (as opposed to the ice phase) without damaging the film quality, even at the very low heating rates employed here (0.5 deg/s). To maintain P(VDF-TrFE) film quality throughout these experiments, the thermal desorption data were not obtained nor shown for temperatures above 410 K, because at temperatures slightly above 410 K, the polymer film begins to degrade with respect to surface quality and remains devoid of defects and pinholes.

We do not believe that the entire film absorbs as much water under the ultrahigh vacuum conditions of these H/D experiments as may occur at higher vapor pressures than undertaken here. Extensive water exposures, as reported in refs 26 and 32, lead to considerable swelling of the PVDF-TrFE films (by several percent). Water absorption undertaken at a vapor pressure of 10^{-6} Torr of water to PVDF-TrFE at 120 K will be limited by the lower bulk diffusivity of water in PVDF-TrFE at 120 K and the smaller vapor pressure. The extent of equilibrium water absorption in PVDF-TrFE under UHV conditions remains to be explored.

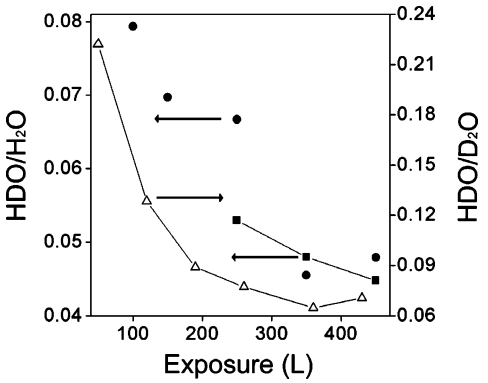

Figure 2. HDO from D_2O and HDO from H_2O production at the ice-to-polymer interface are compared. The ratio of HDO to D_2O for the thermal desoprtion heavy water ice peak (desorbing at about 165 K for both heavy water and HDO) desorption spectra, as a function of D_2O exposure to P(VDF-TrFE) at 120−135 K, is shown (△). The ratio of HDO to H_2O obtained from the water and HDO ice thermal desorption peaks (desorbing at approximately 155 K) are shown as a function of H_2O exposure to P(VDF-TrFE) at 120−135 K (■) along with the water and HDO ratio obtained from the thermal desorption peaks characteristic of absorbed (desorbing at approximately 375 K) (●) from the desorption spectra. The HDO-to-H_2O ratio data were taken after the sample was heavily deuterated through considerable exposure to heavy water over a number of thermal desorption cycles (see text).

5. Isotopic Exchange

To demonstrate that there is isotopic hydrogen exchange between water and the P(VDF-TrFE) polymer, we exposed D_2O to the native nominally 35 ML (≈170 Å) thick undeuterated P(VDF-TrFE) films at 120 to 135 K. Both heavy water (20 amu) and HDO (19 amu) were simultaneously observed in the thermal desorption spectra, as seen in Figure 1, spectra a and b, respectively. The thermal desorption signal of HDO is only about seven times smaller than the one from heavy water D_2O, in Figure 1, giving an indication of the relative amount of HDO produced. This reveals that the isotopic exchange of H/D atoms between heavy water and the polymer monomer (CH_2-CF_2) is surprisingly efficient. This HDO production is evident in the 160 K water ice thermal desorption peak.

While the H/D exchange reaction $H_2O + D_2O \rightarrow 2HDO$, between water molecules[1] and within ice,[2−4] is known, this cannot be the source of HDO production observed here. There is no H_2O available for isotopic exchange. Since the isotopic exchange leading to HDO production must occur with the polymer substrate, continued exposure of PVDF-TrFE to D_2O will lead to the deuteration of PVDF-TrFE.

The ratio of HDO/D_2O (△) decreases with increasing coverage (i.e. as a function of increasing heavy water exposure to P(VDF-TrFE) at 120−135 K). Our data show a greater isotopic exchange rate at lower D_2O exposures and the exchange decreases in proportion to the total amount of heavy water introduced as the ice layer increases, as seen in Figure 2. Thus HDO production must be greater at the D_2O ice−polymer interface, where the $-CH_2-$ polymer groups and D_2O are in closest proximity.

To confirm that the hydrogen/deuterium exchange between water and the copolymer is dominant at the ice−polymer interface, we exposed water to a nominally 35 monolayer thick sample that was significantly deuterated through continued

exposure to D_2O over many thermal desorption and low-temperature exposure treatment cycles. Following exposure of this 35 monolayer P(VDF-TrFE) film at 135 K to H_2O, both H_2O and HDO were observed to evolve simultaneously in the desorption mass spectra, as seen in Figure 1, spectra c and d, respectively. In this case, in Figure 1, the HDO signal is 12 times smaller than the H_2O signal. This is smaller than the corresponding ratio for HDO/D_2O, either as a result of imperfect deuteration of the P(VDF-TrFE) or because hydrogen/deuterium exchange is less efficient for water than for D_2O. In other words, the deuteration of P(VDF-TrFE) resulting from exposure to D_2O can be at least partly "reversed" through the exposure to water as part of taking thermal desorption spectra.

Figure 2 illustrates the ratio of coverage of HDO/H_2O for the bulk absorbed water thermal desorption peak (●) at 365 K and the water ice thermal desorption peak at 155K (■) (as both are easily observed in the thermal desorption of water), as shown in Figure 1c,d, for various exposures of water to P(VDF-TrFE) at 120−135 K. As observed previously for D_2O, the isotopic exchange, as indicated by the ratio of HDO/H_2O, is greater at low water exposures and decreases for larger water exposures, until the sample has been rehydrogenated.

Water and heavy water are in close proximity to $-CH_2-$ polymer groups not only at the surface of the polymer, but also within the polymer bulk as water is absorbed into PVDF-TrFE.[26,32] We have ascertained that H/D exchange does not occur only at the (heavy) water ice to polymer interface but that H/D exchange can occur between absorbed water and the surrounding P(VDF-TrFE) as well. This is established from the HDO evolving in thermal desorption with the water and heavy water desorption peaks, at 365 K and higher. The thermal desorption peaks, at 365 K and higher, are associated with an absorbed water species as noted above.

Thermal desorption experiments were undertaken on a slightly thinner P(VDF-TrFE) film of nominally 25 monolayers (to lower slightly the temperature of the absorbed water thermal desorption peak) and alternating H_2O and D_2O (the alternation of H_2O and D_2O experiments is meant to prevent excessive deuteration or rehydrogenation). Desorption spectra were measured for the HDO (o) and H_2O (●) masses simultaneously, after a H_2O exposure to P(VDF-TrFE) at 120−135 K, and the HDO (o) and D_2O (●) masses simultaneously after D_2O exposure to P(VDF-TrFE) at 120−135 K, plotted as intensities in Figure 3, panels a and c, respectively. The thermal desorption intensities for the bulk absorbed H_2O and D_2O phase that desorbs from P(VDF-TrFE) at higher temperatures (above 300 K) are plotted in Figure 3a,c. Panels b and d in Figure 3 show the ratios for HDO/D_2O and HDO/H_2O as a function of D_2O and H_2O exposure, respectively. As indicated in Figure 3, this more strongly bound water and heavy water species (absorbed water and heavy water) are associated with significant HDO production, i.e., significant isotopic exchange.

6. Modeling of Water Adsorption and H/D Exchange in P(VDF-TrFE) Films

While we cannot identify the mechanism for the origin of the significant H/D exchange between the absorbed water and P(VDF-TrFE) $-(CH_2-CF_2)_7-(CHF-CF_2)_3-$ (70%:30%) from our experimental data, model calculations do suggest a mechanism. We believe that the strong local electric fields in the P(VDF-TrFE) films are responsible for the hydrogen/deuterium exchange between the absorbed water and P(VDF-TrFE) and significant HDO production observed in our thermal desorption measurements. This is consistent not only with the experimental

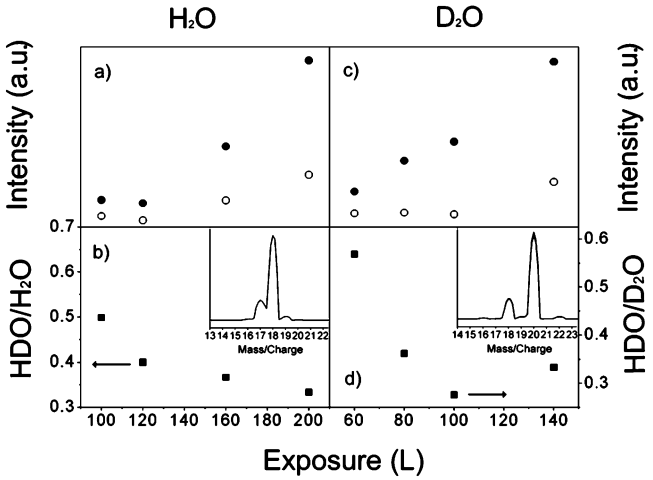

Figure 3. HDO from D_2O and HDO from H_2O production from absorbed heavy water and water are compared. Panels a and b show the integrated intensity of the water (●) and heavy water (■) and the corresponding HDO (○) intensity abstracted from the thermal desoprtion peak associated with absorbed water (desorbing at approximately 375 K) as a function of water or heavy water exposure to P(VDF-TrFE) at 120−135 K. Panels b and d show the coverage of the HDO/H_2O and HDO/D_2O ratios for alternating water and heavy water thermal desorption experiments of as function of exposure of water and heavy water, respectively, to P(VDF-TrFE) at 120−135 K. The insets show the mass spectra of H_2O and D_2O, i.e., no HDO (mass 19) without isotopic exchange with the P(VDF-TrFE).

results just presented, but also with the experimental observation that the addition of HCl to water and heavy water ice films significantly enhances isotopic exchange.[3,4]

To understand the influence of the local dipoles, the interplay between water, the water molecular orientation with respect to the P(VDF-TrFE) molecular orientation has been explored as well. The investigation of the structure of the monolayer P(VDF-TrFE) film on graphite substrate must, nonetheless, be the starting point for understanding the influence of the P(VDF-TrFE) local dipole structure on adsorbed and absorbed water.

6.1. The P(VDF-TrFE) Films on Graphite. The structure of the crystalline P(VDF-TrFE) films on graphite substrate was studied in detail by STM,[36,37] LEED,[39,40] and X-ray diffraction techniques.[26,29] The monolayer adsorbed film consists of long parallel polymer chains with a 3.3 Å period in a direction perpendicular to the chain axes, with hydrogen terminated (hydrophobic) surface. In our simulations, a P(VDF-TrFE) monolayer was modeled by several (up to 4) polymer chains, terminated by hydrogen atoms to saturate dangling bonds at the chain ends (Figures 4a). For the sake of reasonable computation time, the total number of atoms must be restricted, but the number of chains as well as the number of $-(CH_2-CF_2)-$ or $-(HFC-CF_2)-$ fragments adopted for our simulations was deemed sufficient for our model calculations when verified through a comparison of the resulting geometry of the system with the known experimental structure(s). In particular, the calculated periods along the chains (2.57 Å) and between the chains (4.62 Å) are consistent with data obtained in LEED and X-ray diffraction studies of thicker crystalline P(VDF-TrFE) films (2.55 and 4.56 Å, respectively),[36,37] and do not change noticeably when decreasing the number of atoms in simulations.

Results of geometry optimization of the P(VDF-TrFE) monolayer on graphite reveal that the film can be characterized as "floating" above the graphite surface (see Figure 4). In other words, the influence of the graphite substrate on adsorbed film structure is weak (except for the extrinsic influence on dipole ordering[47]). This suggests that the substrate also has little

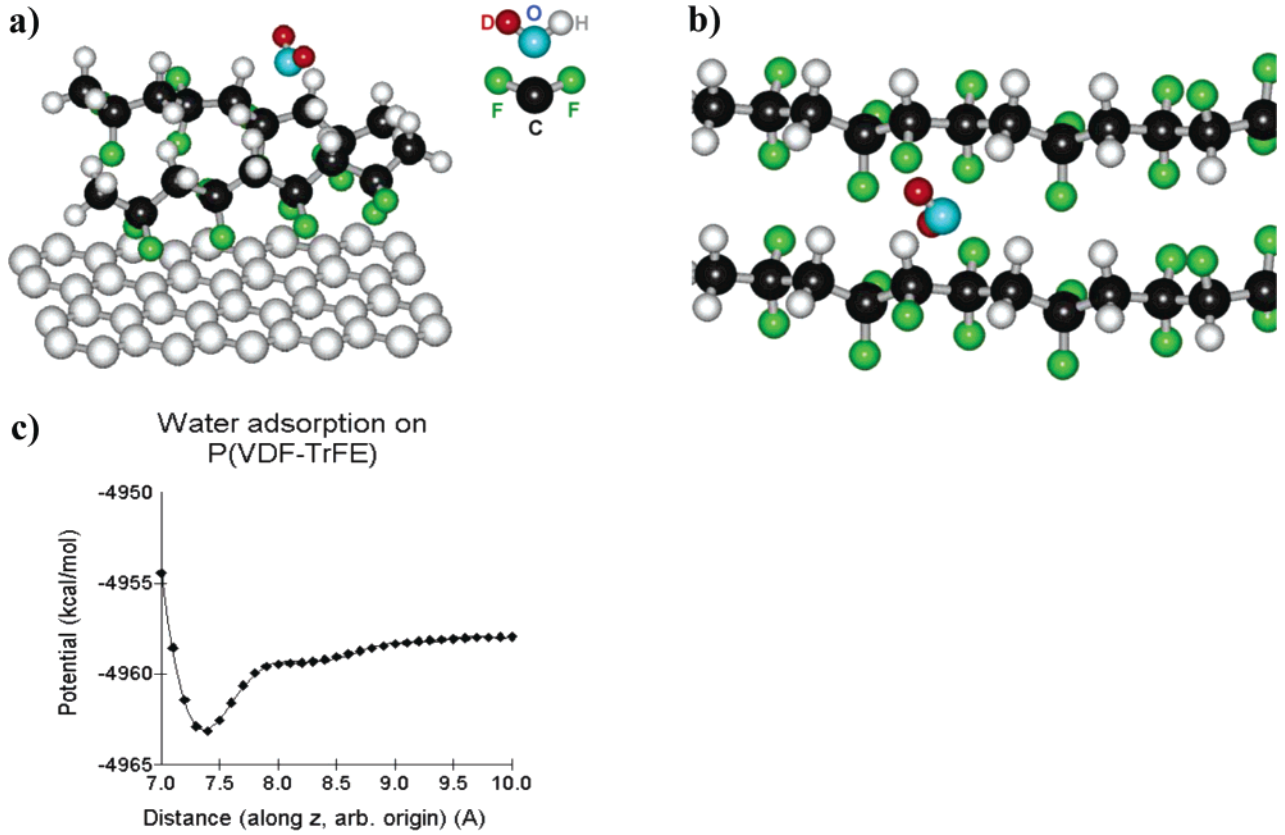

Figure 4. Physisorption of the water molecule at the hydrogen terminated (hydrophobic) P(VDF-TrFE 70:30) surface. The (heavy) water molecule is in a favorable position approximately at 3.5 Å from surface carbon atoms. The hydrogen (or deuterium) atoms of water, which are oriented toward the vacuum ("hands up") upon adsorption on the H-side of the PVDF film on a graphite substrate (shown by gray spheres) (a), reorient toward the F atoms near a TrFE segment within the P(VDF-TrFE) chains (b). In panel c, the potential energy (in kcal/mol) for adsorption of a water molecule is plotted as a function of distance from the P(VDF-TrFE) film along the normal to the surface. (The origin of the *x* axis was arbitrarily chosen below the monolayer, at 4 Å from the C atoms of the CH_2 fragments, so that the minimum at "7.4 Å" is 3.4 Å from C atoms of the hydrophobic surface.) The depth of the potential well is 6 kcal/mol (0.25 eV).

influence on water adsorption on the film surface. The number of the polymer chains and their length, employed in these simulations, were also not especially critical to the outcome of the calculations.

The calculated dipole moment of the $-(CH_2-CF_2)-$ fragment of the PVDF chain is on the order of 1.9 D, a fragment similar to that for water (1.74 D, as noted above). In some cases, the electric field in the ferroelectric P(VDF-TrFE) film, as follows from our molecular dynamics simulations, can lead to a field dissociation of the absorbed water molecule when placed in close proximity to the large dipole from P(VDF-TrFE).

6.2. Physisorption of the Water Molecule on P(VDF-TrFE). In the ferroelectric state, the free open surface of the crystalline copolymer poly(vinylidene fluoride with trifluoroethylene (30%)), P(VDF-TrFE 70:30), is hydrogen terminated,[35,37] and therefore we have concentrated our model calculation efforts to explore a water molecule approaching a hydrogen-terminated (hydrophobic) surface. Equilibration (geometry optimization) of the water molecule near the above two polymer chains (relatively short, that is, built from 4 fragments each) reveals that water adsorbs in a physisorption state, located approximately 3.5 Å from the surface carbon atoms (Figure 4a). There is a preferential bonding orientation of water on the polymer surface: the hydrogen of water, which is oriented toward the vacuum ("hands up") adsorbed on the H-side of the PVDF film, as schematically shown in Figure 4a. The water reorients toward the F atoms near a TrFE segment within the P(VDF-TrFE) chains (Figure 4b).

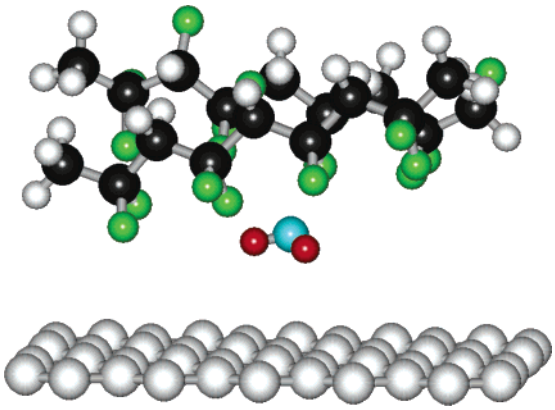

Figure 5. The water molecule in a favorable position between graphite substrate and the F-terminated (hydrophilic) side of the film (see text). Conventions are as in Figure 4.

The depth of the potential well (Figure 5c), which does not depend noticeably on the length of the polymer chains nor the presence of the graphite substrate, is about 6 kcal/mol (0.25 eV). This value for the binding energy appears to be insufficient for an explanation of the 165 K desorption peak by itself (using the empirical Frenkel equation [ref 48], where $E_d \approx T \times (2.6 \times 10^{-3})$, one can roughly estimate the activation energy E_d to be about 0.4 eV from the corresponding temperature T of the desorption peak), but the desorption energy for water from the adsorbed water at the polymer surface must also include the binding energies between coadsorbed and condensed adjacent

water molecules, which are not included here. It seems apparent from experiment that this weakly bound polymer surface water species is little different in desorption energy than water in a multilayer of condensed water.

The significance of this water physisorption potential and the physisorption state, nonetheless, may be very significant because the additional P(VDF-TrFE) to water binding energy could provide some additional ordering to adsorbed water when an ice phase forms at the surface, thus a water contribution to the ferroelectric state may be possible when water is present. These contributions of adsorbed water to the dielectric properties of PVDF-TrFE have been suggested and observed elsewhere.[26]

6.3. Rigid Chains. By plotting the total energy as a function of distance between a water molecule and the P(VDF-TrFE) surface, as shown in Figure 4c, it is clear that there is a very high barrier from the film surface side, which cannot be overcome by even a "hot" water molecule impinging upon the P(VDF-TrFE) surface. (Note that with zero kinetic energy for the impinging water, the total energy becomes equal to the potential energy.) This significant barrier to water absorption is reduced, indeed will be almost completely eliminated, if the crystalline P(VDF-TrFE) film structure is allowed to relax in response to the approach of a water molecule.

This high potential energy region near the surface is predominantly the result of the strong electrostatic field in the vicinity of the hydrophobic side of the polymer film. Hence, if the P(VDF-TrFE) chains remain "rigid" (that is, without any accommodation of the P(VDF-TrFE) chain shape and orientation to the insertion of a water molecule), then water molecules cannot penetrate between neighboring P(VDF-TrFE) chains. In the situation where the chains remain rigid, water absorption (as opposed to adsorption) can only occur as a result of imperfections in the crystalline copolymer film surface.

Between two "rigid" chains of P(VDF-TrFE), our model calculations nonetheless show that water can be absorbed between the polymer chains only in a few special orientations and the potential barrier to water absorption remains too high, about 20 eV. Even if the water molecule absorbs in these "special" positions between P(VDF-TrFE) chains, the total energy would exceed that of the film and evaporated molecule separately. In other words, this position corresponds to a metastable configuration, which hardly could appear in reality.

Should the water succeed in penetrating the surface barrier of a rigid chain structure, then the molecule adopts a very favorable position (energetically) between graphite substrate and the F-terminated (hydrophilic) side of the film (Figure 5). It seems very likely that water can accumulate in this region and could contribute to the thermal desorption spectra at temperatures above 300 K. This is not likely in the experiments reported here, but would be more likely for very thin PVDF-TrFE films on graphite studied elsewhere,[32] and does deserve mention.

6.4. Barriers to Water Absorption with Flexible Polymer Chains. The scanning tunneling microscopy (STM) studies of the PVDF-TrFE polymer surfaces suggest that the polymer chains at the surface are "flexible".[33,34] The vibrational mode studies (high-resolution electron energy loss spectroscopy and high-resolution photoemission) also indicate that, to some extent, the surface is soft.[38] The surface dipoles undergo temperature-dependent dynamic motion.[38] Distortions of the polymer chains must therefore be possible. By allowing the P(VDF-TrFE) chains to adapt their shape and orientation to conform to a strong perturbation resulting from an impinging water molecule, model calculations show that the potential barrier to water absorption decreases significantly.

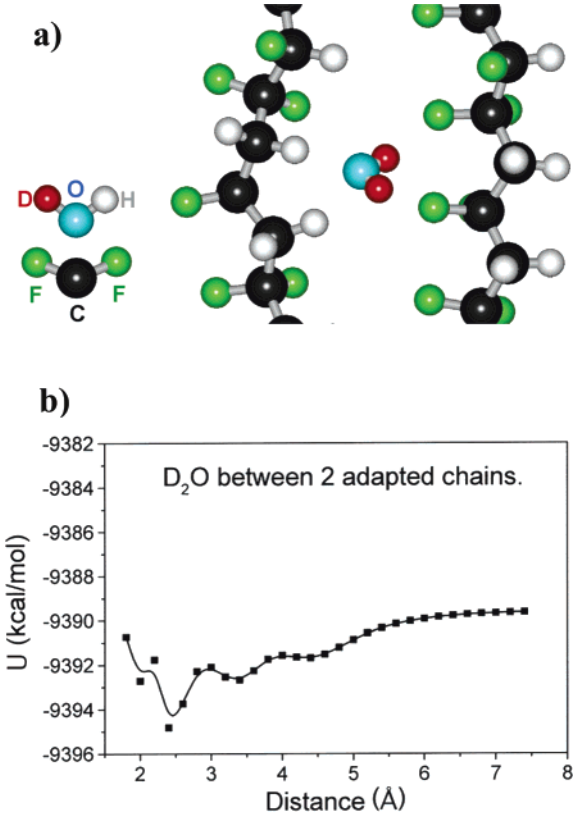

Figure 6. With flexible polymer chains, the (heavy) water molecule can adopt a favorable position between the PVDF chains at the hydrophobic side of the film (a). The lower energy geometry is a result of a strong local distortion of the chains (see text). (b) The one-dimension potential along the surface normal (the origin of the *x* axis is placed at the CF_2 surface of the monolayer). The minimum of the potential at 3.4 Å is an equilibrium stable position for water between $-CH_2-$ units of the adjacent P(VDF-TrFE) chains.

Because of a strong electrostatic field, the total energy depends significantly on the orientation of the water molecule between P(VDF-TrFE) chains. This feature makes the potential energy surface extremely complicated. The usual methods for determination of saddle points in the potential energy surface are impractical. In this situation an evaluation of binding energy can be better accomplished through calculations of potential energy for a given orientation of the water molecule, ideally one that corresponds to the water molecule in the optimized geometry. In Figure 6b, such a one-dimensional potential is presented, along the normal to the surface, for a range of positions (distances) from approximately the favorable water position between the hydrophobic sides of P(VDF-TrFE) chains to a position in the vacuum at sufficient distance from the surface (the *x*-axis origin was chosen, arbitrarily, to be near the F-side of the P(VDF-TrFE) film). The depth of the potential well, about 6 kcal/mol (about 0.25 eV), is consistent with the temperature of the desorption peak at 165 K (see Figure 1).

With flexible polymer chains, the (heavy) water molecule can occupy favorable positions not only near the hydrophilic F-side, but also between the chains at the hydrophobic side (H-side or surface) of the crystalline PVDF-TrFE film (Figure 6a). This favorable absorbed water geometry is a result of a strong local distortion of the PVDF-TrFE chains. Consider the response of two parallel PVDF-TrFE chains to the presence of a water molecule: while the left chain (in Figure 6a) has become curved, the right chain rotates along its axis to turn the fluorine ends toward H (D) atoms of the water (heavy water) molecule. It

should be noted that this water position between two P(VDF-TrFE) chains corresponds to a kind of intermediate state between adsorption and absorption in the bulk P(VDF-TrFE).

The one-dimensional potential from the equilibrated position for a water molecule at the hydrophobic side (of the P(VDF-TrFE) copolymer) toward vacuum (in Figure 6b) seems reasonable because of the very small dependence of the total energy on the water molecule orientation when placed outside the film. This is not the case inside the P(VDF-TrFE) film. The free P(VDF-TrFE) polymer surface interaction with water does differ from the bulk interaction of PVDF-TrFE with water, as indicated above, but the type of PVDF-TrFE surface is also a consideration. This is easily seen by noting that the interactions with water on the fluorine (hydrophilic) side of the polymer differ from those of the hydrogen (hydrophobic) side.

A water molecule can adopt an even lower energy configuration at the hydrophilic F-side of P(VDF-TrFE) than at the H-side. Following a trajectory for the absorbed water molecule, from inside the film toward the hydrophilic F-side of P(VDF-TrFE), barriers (effectively barriers to diffusion) do exist, but the migration of water is facilitated significantly by a proper orientation of the water molecule at each point of the trajectory. A number of possible trajectories were analyzed for a water molecule positioned somewhere about the center of the film for a trajectory between the chains. These simulations suggest that flexible chains, which respond to an approaching water molecule, lower the potential barriers to water absorption. This is particularly true if the water molecule orientation is not fixed, i.e., has no a priori orientation, as would be the case in experiment. From inside the film toward the hydrophilic F-side of P(VDF-TrFE), the film is partly transparent with respect to the migration of water even when simulations were performed at temperatures as low as 100 K.

From inside the film toward the hydrophobic H-side of the P(VDF-TrFE) film, the water mobility is found to be appreciable at higher temperatures approaching 300 K. This is partly the basis for our suggestion that there is no equilibrium of the absorbed water throughout the PVDF-TrFE film following exposure to water at 120 K, as noted in section 4.

The fact that water does not want to penetrate into P(VDF-TrFE) unless a surface defect is encountered or some event, such as the much slower adaptation of chains to electrostatic potential of the molecule, occurs thus allows the water to be more readily absorbed. This is consistent with earlier X-ray diffraction studies, of water absorption by P(VDF-TrFE),[26] which suggested a barrier to water absorption but facile diffusion of water within the crystalline copolymer matrix. This can also be reconciled with the thermal desorption data where water absorption occurs prior to the formation of a water ice on the surface of P(VDF-TrFE).

When a water molecule approaches the surface, a high potential barrier at the surface prevents the water molecule from penetrating into the film. At low temperatures, such a molecule, reflected from the surface, can, nonetheless, be captured in the physisorption state (though, perhaps, probability of physisorption may remain rather small). The weakly adsorbed surface water species acts as a precursor state[48] to absorption. Water molecules with the proper orientation can approach more closely to the polymer surface between the polymer chains and cause chain distortion by proximity. The chain distortion eliminates the potential barrier for water molecule absorption, which can then be "adsorbed" at the H-side of the copolymer films and, very likely, would then migrate further into the film to occupy an energetically favorable position near the hydrophilic F-side.

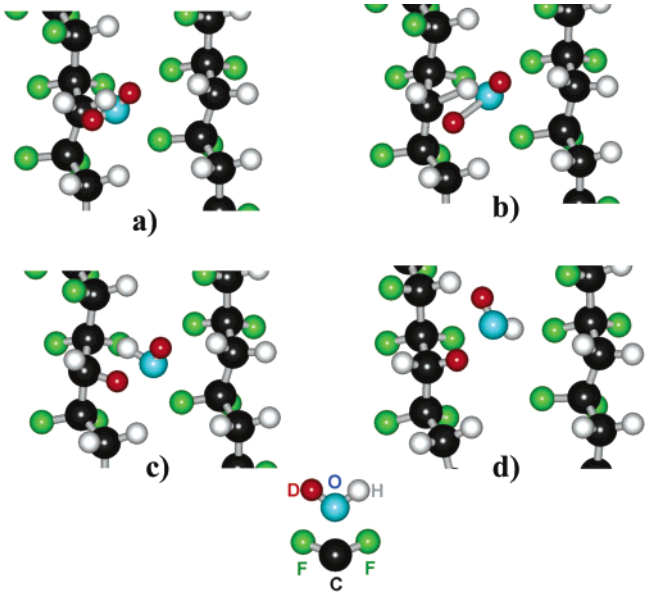

Figure 7. The H/D exchange mechanism is illustrated by "snapshots" is illustrated. When a D_2O molecule occurs close enough to a $-CH_2-$ unit of the P(VDF-TrFE) chain (a), a D atom substitutes an H atom in the fragment, while the H atom is captured by the DO group (b, c). Subsequent evaporation of the HDO molecule is accompanied by relaxation of the chain structure (d).

After one water molecule passes through the surface P(VDF-TrFE) layer, the polymer PVDF-TrFE chains will relax back into their initial shape. This chain relaxation, however, is relatively slow compared to the speed of water molecules at finite temperature and this is evident in the molecular dynamics simulations. The slow relaxation of the P(VDF-TrFE) chains, after the passage of the water molecule, can be easily understood. The chain distortion relaxation to an equilibrium "straight" chain configuration involves the motion of rather long fragments of the PVDF-TrFE chains (so the mass of the water molecule is significantly less than the mass of the shifted fragments). This "persistent" distortion of the P(VDF-TrFE) chains means that the barriers for absorption of another incoming water molecule remain low for a considerable time. In other words, the first (lucky) molecule distorts the chains and thus "opens" a pathway for other water molecules.

A loss of chain order, due to water absorption within crystalline copolymer poly(vinylidene fluoride with trifluoroethylene (30%)), P(VDF-TrFE 70:30), is indicated in our model calculations as a result of the distortion of the chains in close proximity to a water molecule. This is in good agreement with the observed decrease in the X-ray diffraction P(VDF-TrFE 70:30) ⟨110⟩ direction layer spacing intensity that accompanies water absorption.[32,38]

6.5. Hydrogen/Deuterium Exchange. The strong distortion of the polymer chains, obviously, originates from electrostatic interaction between the ferroelectric P(VDF-TrFE) copolymer film and the water molecule. It seems very likely that the electric field in the film will facilitate the hydrogen exchange between the water molecule and P(VDF-TrFE). Indeed, if a heavy water molecule is placed in sufficiently close proximity to the $-CH_2-$ fragment of the P(VDF-TrFE) chain (Figure 7a), then the D−O bond becomes significantly weaker and the D/H exchange between the $-CH_2-$ fragment and D_2O molecule becomes possible.

The process of the isotopic exchange of this type is illustrated by snapshots obtained in the course of geometry optimization (or, equivalently, molecular dynamic (MD) simulations with a

"fast" relaxation to the thermostat temperature of 300 K), as shown in Figure 7. When a D_2O molecule approaches close enough to a $-CH_2-$ fragment of the P(VDF-TrFE) chain (Figure 7a), a D atom substitutes for an H atom in the fragment, while the H atom is captured by the DO group (Figure 7b,c). The subsequent evaporation of the HDO molecule is accompanied by the relaxation of the chain structure, now with a $-CHD-$ fragment instead of a $-CH_2-$ fragment (Figure 7d).

7. Summary

There is significant H/D exchange between absorbed heavy water and the crystalline copolymer poly(vinylidene fluoride with trifluoroethylene (30%)), P(VDF-TrFE 70:30), as summarized in Figure 3. This work also illuminates a method for the deuteration of partially fluorinated polymers (and no doubt many other polymers as well) by exploiting the efficient isotopic exchange between heavy water and the crystalline copolymer poly(vinylidene fluoride with trifluoroethylene (30%)), P(VDF-TrFE 70:30), in other like polymers.

We suggest, based on our model calculations, that there are several adsorption sites between absorbed water and surface water ice that can form on the polymer surface. There is an adsorption site for water molecules at the hydrophobic H-side of the film, which also could contribute to the 165 eV peak in TPD spectra associated with the desorption of water. Capturing a D_2O molecule in this latter state will inhibit the H/D exchange between the molecule and $-CH_2-$ units within the polymer chains.

The suggestion of a strong barrier to water absorption and a water absorption induced distortion of the crystalline P(VDF-TrFE 70:30) chains, obtained from molecular mechanics calculations, does much to explain prior X-ray diffraction studies of water absorption.

Small dipolar molecules are strongly influenced by the defects and dipoles at the surfaces of ferroelectrics[49−51] with indications that the ferroelectric dipole reordering affects molecular desorption from both organic[32] and inorganic[50,51] ferroelectrics. The Teflon-like polymer poly(vinylidene fluoride) (PVDF) and its copolymers with trifluoroethylene (TrFE), as well as tetrafluoroethylene, has many advantages for the study of such adsorbate interactions with substrate ferroelectric dipoles as this system (although a polymer) does not exhibit surfaces with as many complexities as observed for the inorganic ferroelectric surfaces (defects, segregation of constituents, etc.). The observation of H/D exchange and the apparent "flexibility" of the polymer surface chains are, nonetheless, additional complexities to be considered in adsorbate interactions with organic ferroelectrics.

Acknowledgment. This work was supported by the National Science Foundation through grant CHE-0415421. The authors are grateful to S. Ducharme, C. Othon, and M. Poulsen for access to their sample fabrication facilities, and to P. Jacobson for his technical assistance.

References and Notes

(1) Ryan, P. W.; Blakey, C. R.; Vestal, M. L.; Futrell, J. H. *J. Phys. Chem.* **1980**, *84*, 561. Smith, D.; Adams, N. G.; Hechman, M. J. *J. Chem. Phys.* **1980**, *72*, 4951. Adams, N. G.; Smith, D.; Hechman, M. J. *Int. J. Mass Spectrom. Ion Phys.* **1982**, *42*, 11. Del Bene, J. E.; Frisch, M. J.; Pople, J. A. *J. Chem. Phys.* **1985**, *89*, 3669. Hechman, M. J.; Paulson, J. F. *J. Chem. Soc. Faraday Trans. 2* **1989**, *85*, 1673. Hechman, M. J.; Smith, D.; Adams, N. G. *Int. J. Mass* Spectrom. *Ion Proc.* **1991**, *109*, 105. Anicich, V. G.; Sen, A. D. *Int. J. Mass Spectrom. Ion Proc.* **1998**, *172*, 1. Rheinecher, J.; Xie, T.; Bowman, J. M. *J. Chem. Phys.* **2004**, *120*, 7018. Honma, K.; Armentrout, P. B. *J. Chem. Phys.* **2004**, *121*, 8307.

(2) Ritzhaupt, G.; Thornton, C.; Devlin, J. P. *Chem. Phys. Lett.* **1978**, *59*, 420. Ritzhaupt, G.; Devlin, J. P. *Chem. Phys. Lett.* **1979**, *65*, 592. Ritzhaupt, G.; Devlin, J. P. *J. Chem. Phys.* **1980**, *72*, 6807. Thornton, C.; Khatkale, M. S.; Devlin, J. P. *J. Chem. Phys.* **1981**, *75*, 5609. Bertie, J. E.; Devlin, J. P. *J. Chem. Phys.* **1983**, *78*, 6203. Collier, W. B.; Ritzhaupt, G.; Devlin, J. P. *J. Phys. Chem.* **1984**, *88*, 363. Wooldridge, P. J.; Devlin, J. P. *J. Chem. Phys.* **1988**, *88*, 3086. Livingston, F. E.; Whipple, G.; George, S. *J. Chem. Phys.* **1998**, *108*, 2197. Devlin, J. P.; Joyce, C.; Buch, V. *J. Phys. Chem. A* **2000**, *104*, 1974. Uras-Aytemiz, N.; Joyce, C.; Devlin, J. P. *J. Chem. Phys.* **2001**, *115*, 9835. Devlin, J. P.; Sadlej, J.; Buch, V. *J. Phys. Chem. A* **2001**, *105*, 974.

(3) Livingston, F. E.; George, S. *J. Phys. Chem. B* **1999**, *103*, 4366. Everest, M. A.; Pursell, C. *J. Chem. Phys*. **2001**, *115*, 9843;

(4) Park, Seon-Chang; Jung, K. H.; Kang, H. *J. Chem. Phys.* **2004**, *121*, 2765.

(5) Takayanagi, T.; Masaki, N.; Nakamura, K.; Okamoto, M.; Sato, S. *J. Chem. Phys.* **1987**, 11, 6133. Mitchell, N.; LeRoy, D. J. *J. Chem. Phys.* **1973**, *58*, 3449. Westenberg, A. A.; de Haas, N. *J. Chem. Phys*. **1967**, *47*, 1393.

(6) Bonhoeffer, K. F.; Klar, R. *Naturwissenschaften* **1934**, *22*, 45.

(7) Hvidt, A.; Linderstom-Lang *Biochim. Biophys. Acta* **1954**, *14*, 574. Hvidt, A.; Linderstom-Lang *Biochim. Biophys. Acta* **1955**, *16*, 168. Kaltashov, I. A. *Int. J. Mass Spectrosc*. **2005**, *240*, 249. Engel, M. F. M.; Visser, A. J. W. G.; Mierlo C. P. M. *Proce. Natl. Acad. Sci. U.S.A.* **2004**, *101*, 11316.

(8) Gabelica, V.; Rosu, F.; Witt, M.; Baykut, G.; De Pauw, E. *Rapid Commun. Mass Spectrom*. **2005**, *19*, 201.

(9) Thiel P. A.; Madey T. E. *Surf. Sci. Rep.* **1987**, *7*, 211.

(10) Henderson, M. A. *Surf. Sci. Rep.* **2002**, *46*, 5.

(11) Briggs, D. *Surface Analysis of polymers by XPS and static SIMS*; Clarke, D. R., Suresh, S., Ward, I. M., Eds.; Cambridge Solid State Science Series; Cambridge University Press: Cambridge U.K., 1998; p 6 "...there are a few definitive studies of the polymer surface structure−property relationships".

(12) Chen, X.; Gardella, J. A.; Ho, T.; Wynne, K. *J. Macromolecules* **1995**, *28*, 1635.

(13) Toselli, M.; Messori, M.; Bongiovanni, R.; Malucelli, G.; Priola, A.; Pilati, F.; Tonelli, C. *Polymer* **2001**, *42*, 1771.

(14) Chen, J. X.; Zhuang, H. Z.; Zhao, J.; Gardella, J. A. *Surf. Interface Anal*. **2001**, *31*, 713.

(15) Gardella, J. A.; Mahoney, C. M. *Appl. Surf. Sci.* **2004**, *231/2*, 283.

(16) Toselli, M.; Gardella, J. A.; Messori, M.; Hawkridge, A. M.; Pilati, F.; Tonelli, C. *Polym. Int.* **2003**, *52*, 1262.

(17) Opdahl, A.; Phillips, R. A.; Somorjai, G. A. *J. Polym. Sci. Part B* **2004**, *42*, 421.

(18) Lewis, K. B.; Ratner, B. D. *J. Colloid Interface Sci.* **1993**, *159*, 77.

(19) Yasuda, T.; Miyyama, M.; Yasuda, H. *Langmuir* **1994**, *10*, 583.

(20) Hawkridge, A. M.; Gardella, J. A.; Toselli, M. *Macromolecules* **2002**, *35*, 6533.

(21) Lee, S. H.; Ruckenstein, E. *J. Colloid Interface Sci.* **1987**, *120*, 529.

(22) Lukás, J.; Sodhi, R. N. S.; Sefton, M. V. *J. Colloid Interface Sci.* **1995**, *174*, 421.

(23) Yasuda, H.; Okuno, T.; Sawa, Y.; Yasuda, T. *Langnuir* **1995**, *11*, 3255.

(24) Ruckenstein, E.; Gourisankar, S. V. *J. Colloid Interface Sci.* **1985**, *107*, 488.

(25) Ruckenstein, E.; Gourisankar, S. V. *J. Colloid Interface Sci.* **1986**, *109*, 557.

(26) Jacobson, P. A.; Rosa, L. G.; Othon, C. M.; Kraemer, K. L.; Sorokin, A. V.; Ducharme, S.; Dowben, P. A. *Appl. Phys. Lett.* **2004**, *84*, 88.

(27) Castela, A. S.; Simoes, A. M. *Corros. Sci.* **2003**, *45*, 1631.

(28) Castela, A. S.; Simoes, A. M. *Corros. Sci.* **2002**, *45*, 1647.

(29) Furukawa, T. *Phase Trans.* **1989**, *18*, 143.

(30) Blinov, L. M.; Fridkin, V. M.; Palto, S. P.; Bune, A. V.; Dowben, P. A.; Ducharme, S. *Usp. Fiz. Nauk* **2000**, *170*, 247−262; *Phys.-Usp.* (*Engl. Transl.*) **2000**, *43*, 243−257.

(31) Ducharme, S.; Palto, S. P.; Fridkin, V. M. *Ferroelectric Polymer Langmuir−Blodgett Films. Handbook of Surfaces and Interfaces of Materials*; Vol. 3, Ferroelectric and Dielectric Films; Academic: Sandiego, CA, 2001; Chapter 11, pp 546−592.

(32) Rosa, L. G.; Jacobson, P. A.; Dowben, P. A. *J. Phys. Chem. B* **2005**, *109*, 532.

(33) Qu, H.; Yao, W.; Garcia, T.; Zhang, J.; Ducharme, S.; Dowben, P. A.; Sorokin, A. V.; Fridkin, V. M. *Appl. Phys. Lett.* **2003**, *82*, 4322.

(34) Cai, L.; Qu, H.; Chenxi Lu, C.; Ducharme, S.; Dowben, P. A.; Zhang, J. *Phys. Rev. B* **2004**, *70*, 155411.

(35) Choi, J.; Dowben, P. A.; Pebley, S.; Bune, A.; Ducharme, S.; Fridkin, V. M.; Palto S. P.; Petukhova, N. V. *Phys. Rev. Lett.* **1998**, *80*, 1328−1331.

(36) Choi, J.; Dowben, P. A.; Ducharme, S.; Fridkin, V. M.; Palto, S. P.; Petukhova, N.; Yudin, S. G. *Phys. Lett. A* **1998**, *249*, 505.

(37) Choi, J.; Borca, C. N.; Dowben, P. A.; Bune, A.; Poulsen, M.; Pebley, S.; Adenwalla, S.; Ducharme, S.; Robertson, L.; Fridkin, V. M.; Palto, S. P.; Petukhova, N.; Yudin, S. G. *Phys. Rev. B* **2000**, *61*, 5760.

(38) Rosa, L. G.; Losovyj, Ya. B.; Choi, J.; Dowben, P. A. *J. Phys. Chem. B* **2005**, *109*, 532.

(39) Borca, C. N.; Welipitiya, D.; Dowben, P. A.; Boag, N. M. *J. Phys. Chem. B* **2000**, *104*, 1047.

(40) Stewart, J. J. P. *J. Comput. Chem*. **1989**, *10*, 209. Stewart, J. J. P. *J. Comput. Chem*. **1989**, *10*, 221.

(41) Chambers, D. K.; Karanam, S.; Qi, D.; Selmic, S.; Losovyj, Ya. B.; Rosa, L. G.; Dowben, P. A. *Appl. Phys. A* **2005**, *80*, 483−488.

(42) Feng, D.-Q.; Caruso, A. N.; Schulz, D. L.; Losovyj, Ya. B.; Dowben, P. A. Thermochromism Effects in Polythiophenes with Pendant Groups. *J. Phys. Chem. B.* Submitted for publication.

(43) Perdew, J. P.; Burke, K.; Ernzerhof, M. *Phys. Rev. Lett.* **1966**, *77*, 3865.

(44) Segall, M. D.; Lindan, P. J. D.; Probert, M. J.; Pickard, C. J.; Hasnip, P. J.; Clark, S. J.; Payne, J. *Phys. Condens. Matter* **2002**, *14*, 2717.

(45) King, D. A. *Surf. Sci.* **1975**, *47*, 384. King, D. A. *Surf. Sci.* **1977**, *64*, 43. Grunze, M.; Strasser, G.; Golze, M.; Hirschwald, W. *J. Vac. Sci. Technol. A* **1987**, 5, 527.

(46) Choi, J.; Tang, S.-J.; Sprunger, P. T.; Dowben, P. A.; Fridkin, V. M.; Sorokin, A. V.; Palto, S. P.; Petukhova, N.; Yudin, S. G. *J. Phys.: Condens. Matter* **2000**, *12*, 4735−4745.

(47) Duan, C.-G.; Mei, W. N.; Yin, W.-G.; Liu, J.; Hardy, J. R.; Ducharme, S.; Dowben, P. A. *Phys. Rev. B* **2004**, *69*, art. no. 235106.

(48) Roberts, M.; McKee, C. S. *Chemistry of the metal-gas interface*; Clarendon Press: Oxford, UK, 1978.

(49) Cabrera, A. L.; Vargas, F.; Zarate, R. A.; Cabrera, G. B.; Espinosa-Gangas, J. *J. Phys. Chem. Solids* **2000**, *62*, 927.

(50) Cabrera, A. L.; Tarrach, G.; Lagos, P.; Cabrera, G. B. *Ferroelectrics* **2002**, *281*, 53.

(51) Parravano, G. *J. Chem. Phys.* **1952**, *20*, 342.